J. Mater. Shaping Technol. (1989) 6:181–193


# Formability and Uniformity Aspects in Drawbead Controlled Geometries

M. Karima and W. Tse

**Abstract.** This paper examines the role of drawbead design within tooling design and stamping engineering, as a system. A microcomputer based program DRAWBD is used to illustrate the effect of tooling adjustments beyond and within the trim line, the variability of material and lubricant on the part thickness, as well as stress and moment distributions.

The paper illustrates that the interactions between the different tooling and operational parameters are very complex, and demonstrates the difficulty in troubleshooting drawbead controlled stamping systems. The conclusion is that the goal in stamping should be to maintain control over the tooling, process, and material windows, and accordingly over uniformity and consistency of interacting parameters.

## INTRODUCTION

Sheet metal engineering is an iterative and interactive process. It is a process that includes, among other things, material selection, process design, tooling design, and the setup of press lines.

During sheet metal forming, it is often necessary to control the rate of metal flow into the die cavity. The control of metal flow can be achieved through the blankholder, lubricant, flange shape, drawbead, or a combination. When flat blankholders are used, the restraining force is largely friction. In stretch forming applications, the role of control or restraining beads is to provide enough tension to deform the material plastically over the punch face, and to ensure proper shape fixing of the part. Beads are also used to restrain and hold back the material at locations of reverses, as with the case of multibottom shells, as well as provide force to stretch any unsupported wall in order to reduce springback.

The use of drawbeads often reduces the amount of blankholding pressure required to draw box shaped parts, and hence increases the drawability limit. In some applications, beads are used to change the metal flow pattern to increase formability. Beads can also be used to deflect metal in some localized areas to prevent metal wrinkling or surface defects. The elongation of the part after passing the drawbead is generally large, though tension is small, with sometimes extreme thickness reduction.

The bead restraining force plays a significant role, affecting the part formability. Beads are an integral part of the tooling design, and should not be designed independently of the other tooling parameters. It is the combination of the drawbead geometry, location, back tension on bead, blankholding force, punch and die profile radii, lubrication, and wall taper angle that dictates the formability of the part.

Hasek [1] has provided considerable experimental data on the load and thickness distribution for strips passing through the drawbeads. Kojima et al. [2] described an analysis of the blankholder load necessary to overcome the bead lifting force, for a circular die with drawbeads. Weidemann [3] postulated that the friction conditions, as affected by the blankholding force, properties of the lubricant, and the sliding speed have the greatest influence on the braking action of a drawbead.

Nine [4] designed a drawbead simulator and was able to separate the deformation force component from the friction component. Nine found that the deformation component is larger than the friction component, accounting for 65 to 85% of the total drawbead restraining force, for normal lubrication conditions [4]. Based on this conclusion, Nine [5] developed the SHAPEMATE insertable drawbead. Nine [6] also ex-

Medhat Karima and William Tse are with the Ontario Centre for Advanced Manufacturing, 400 Collier MacMillan Drive, Cambridge, Ontario, Canada L1R 7H7.

tended his work to cases where Coulomb's friction law breaks down.

Wang [7] developed a plane strain rigid plastic mathematical model for the drawbead restraining force. The deformed sheet is assumed to consist of straight and circular segments, with the latter being conformed to the bead radius. In each curved segment, the deformation is divided into three distinctive processes, bending at the profile radius followed by sliding over the radius and unbending away from it. The convected sheet normals are assumed to remain normal, resulting in simple representation for the tangential velocity distribution across the sheet thickness. The sheet material is assumed to be rate independent and satisfies Hill's anisotropic yield criterion [8].

A drawbead simulator, which incorporates the die shoulder radius, and which is able to draw the specimen in various directions, is described by Furubayashi et al. [9]. A mathematical model was also developed in [9] to predict the elongation at the side wall and the elongation at punch face, as well as elongation of the material passing the drawbead.

Levy [10] used a regression model and the principles of virtual work to formulate the equations for the bead restraining force; the parameters in these equations were determined from the values for the drawing forces measured by Nine [4]. Yellup [11] provided a model for the calculation of the bead parameters, as well as the die opening force. He pointed out that the drawing stress varies linearly with the thickness, and accordingly the force varies as the square of the thickness.

A one-dimensional plane strain, finite strain elastoplastic shell model of the drawbead was developed by Triantafyllidis et al. [12]. They found that the friction coefficient, as compared to geometric and material changes, has little effect on the restraining force and on the sheet failure at the pulling phase. The results of the work compared well to the experiments of Maker et al. [13], except in two cases; as the punch reaches the locked condition, and in the initial stages of pulling deformation.

The sheet metal engineering process is now being recognized within a system's perspective. A list of some of the identified system parameters is given in reference [14]. The system is interactive and generally is considered to have five components—part design, die design, material, lubricant, and press [15,16].

Because the same part can be produced by different processes and process plans, specific strain distributions are rarely specified in the stamped part. It follows from this practice, that material can fail to form satisfactorily not because it is out of specification, but because it differs from that material for which the tooling was first adjusted. Thus problems of *formability* are often confused with lack of *uniformity*. Recent experiences have indicated that improved consistency of the process parameters, such as lubricant, is as much desirable as a goal as the improved consistency of steel or process. The first principle of Statistical Process Control is to control process. Within this process control methodology, better quality steel is being rejected, for being out of specification, for the press setup. The main theme of the paper is to illustrate quantitatively the difference between formability and uniformity related problems, for parts whose formability is controlled by drawbeads.

This paper examines the role of drawbead design within the tooling design and stamping engineering system. It is shown that the drawbead, die, and punch geometries, and tooling operational parameters are interactive within the tooling design system. A micro-based drawbead design and analysis software system DRAWBD is used to illustrate the effects the tooling design and tooling operational parameters have on the final part characteristics. DRAWBD is an interactive computer program to analyze tooling designs and stamping operational conditions for parts, in which the tension of the part walls is controlled by drawbeads. DRAWBD formulation for bending, unbending, and friction is essentially based on Wang's model [7]. However, the approach is generalized to cover practical aspects of bead design such as analysis, springback, and blank development on the whole section covering drawbead, drawdie, punch corner, and punch face as shown in Figure 1. For a given bead, punch and die geometries, friction coefficients, and material properties, DRAWBD calculates the minimum blankholder force required to overcome the bead uplifting force, the force required to sink the bead in, the thickness distribution across the part, as well as the distribution of tension along the part geometry. The program also displays, for each bending and unbending, the through-thickness stress distribution, the location of the neutral axis, the tensional force, the bending moment, the incremental thickness strain, and the total strain distribution across the sheet. Knowledge of the relationship between different tooling and operational parameters is essential in choosing the most suitable drawbead configuration. DRAWBD also allows the prediction of the effect of changes in the drawbead operational conditions, such as coil-to-coil variations in sheet thickness or temper, on the response of the final part.

The formulation of DRAWBD is presented in the next section, together with a critical evaluation of DRAWBD predictions. The paper then illustrates the use of DRAWBD in the tooling design and stamping operational environment.

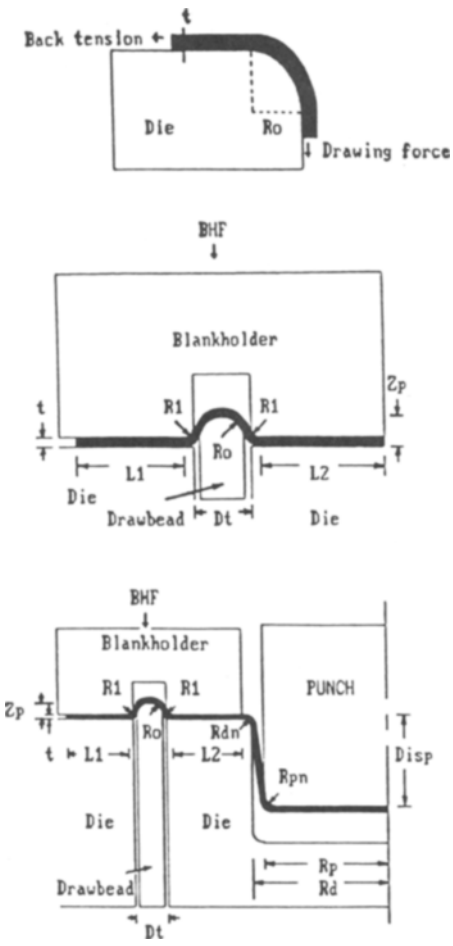


**Fig. 1.** Tooling configurations analyzed by DRAWBD.

## DRAWBD FORMULATION AND TOOLING DESIGN PARAMETERS

The general methodology for the design of drawbeads within the tooling system is described in this section. Drawbeads are designed to provide a tension level at the wall of the die cavity and over the punch face. The practice of the tooling industry is to use standard beads, and then to adjust the tooling parameters and the boundary conditions to obtain an acceptable part. This shows that the problem for the tool designer is not so much to analyze the forming process and determine the stress distribution that results from a given set of boundary conditions, but rather to devise the boundary conditions that will make it reasonably possible for the sheet to deform to the final shape without gross failure [17]. The drawbead tooling and control parameters are:

- blankholder force to sink the beads in place
- blankholder force to overcome the bead lifting force
- blankholder radii, and clearance with bead
- punch and die profile radii
- bead geometry and height (penetration)
- lubrication at punch and die
- position of drawbead
- shape and size of blank, which creates a back tension in flange

The blankholder load should be sufficient to ensure the beads are not forced open during the press stroke, and thus decreasing their restraining force. On the other hand, a large blankholder load would increase the interfacial pressure between the strip and the drawbead surfaces, which is a major factor in determining the material thinning and the rate of wear of the tooling surfaces. The interfacial pressure can also give a good indication of the galling tendencies of the bead system.

The amount of draw as opposed to stretch, as reflected on the die impact line, is a direct reaction to all the tooling and control parameters identified above. The part reaction to a tooling change can be evaluated by careful examination of the thickness distribution, the through-thickness hardness distribution, the location of neutral axis, and the tension and bending moment distributions. This information is used to predict the margin of safety in forming the part, as well as springback. Knowledge of the relationships between the tooling parameters as well as the operational parameters and the part reaction would be valuable in deciding what changes should be made to a bead, boundary control, and tooling system, when the stamping conditions of a part are changed, such as due to the variability of material thickness, temper or due to change of the lubricant. In addition, as large elongations are always found in the material passing through the drawbeads, it appears that deformation analysis of the beads within the tooling system is necessary to improve the accuracy of any forming simulation in the die cavity, and for the prediction of the developed blank shape.

With the above perspective in mind, the DRAWBD software was designed. The program is developed to analyze the three tooling configurations shown in Figure 1. The inputs to the program are the drawbead geometry, punch and die parameters, friction at punch and die, as well as the sheet properties. A typical list of inputs is described in Table 1. The program is flexible in the sense that the different bead radii may be varied independently, with the capability to model any number of bends and unbends as well as any bead configuration. The program also accepts values for the back tension on the bead. The back tension is defined as any force acting on the material entering the bead. This force can be due to a blankholder frictional com-

**Table 1.** List of Input Parameters for DRAWBD

| | |
|---|---|
| Stress constant of material | 77 ksi |
| Yield stress of material | 28 ksi |
| Strain hardening index | 0.22 |
| Friction coefficient of drawbead and die corner | 0.1 |
| Anisotropy parameter | 1.7 |
| Initial sheet thickness, *t* | 0.04 in. |
| Drawbead radius, *Ro* | 0.25 in. |
| Blankholder radius, *R*1 | 0.125 in. |
| Contact length before bead, *L*1 | 1 in |
| Contact length after bead, *L*2 | 1 in. |
| Bead opening, *Dt* | 0.588 in. |
| Drawbead displacement, *Zp* | 0.31 in. |
| Assumed BHF/unit width | 500 lb/in. |
| Assumed initial back tension, *B.T.* | 0 lb/in. |
| Friction coefficient of punch corner | 0.15 |
| Die radius, *Rd* | 4 in. |
| Die corner radius, *Rdn* | 0.25 in. |
| Punch radius, *Rp* | 3.94 in. |
| Punch nose radius, *Rpn* | 0.375 in. |
| Punch displacement, *Disp* | 1.1 in. |

ponent, caused by another bead, or due to a force required to deform the material before reaching the bead location. The force required to deform the material in the flange, for parts deformed in a drawing mode, is calculated from a separate computer program MIDFC [18].

Based on the input, the user is prompted with the wrap angle, around bead, punch and die radii, an approximate minimum blankholder force required to overcome the bead lifting force, and the bead sink-in force. The sink-in force is calculated by equating the blankholder external work done during the sheet displacement to the internal work done to bend the sheet through plastic hinges, to conform to the bead geometry. The approximate minimum blankholder force is calculated through iteration, by first assuming a value for the blankholder force and calculating the corresponding average blankholder pressure. By assuming Coulomb's law of friction the back tension on the bead is evaluated, and by carrying the belt friction assumption through all the bends and unbends, an approximate value for the tension distribution is calculated. The vertical components of the tensions is the bead lifting force. The program accepts any value for the blankholder force, as long as it is larger than the suggested minimum value.

With this new value of the blankholder force, the sheet is bent and unbent, three times for circular beads. The bending, unbending and frictional models are mainly based on Wang's model [7]. The details of the formulation and the numerical procedures can be consulted in the original work of Wang. Based on extensive numerical experiments and different numerical iteration and interpolation algorithms, aimed at optimizing the computer response time, it was found that an optimum solution will be based on 20 elements across the sheet thickness, while each bend or unbend is performed in five incremental steps. After completion of the calculations for the drawbead, the program evaluates again the bead lifting force, and would automatically iterate, should the bead lifting force be larger than the applied blankholder force. The bead restraining force is then used in the calculation of the material thinning and increase in tension at the die radius. This establishes the tension in the die cavity, which is balanced by the reaction at the punch radius. A schematic of DRAWBD is seen in Figure 2.

An enlarged section of the drawbead as analyzed in DRAWBD is shown in Figure 3. The bead restraining load starts to build up from the back tension at the entrance of the bead to a value where the material has completed its traverse across the bead (from A to F as indicated in Figure 3). The formulation implies that the bending and unbending occur at discrete steps at entry and exit from the radius of bend, and not in a smooth and transitional manner along the bend

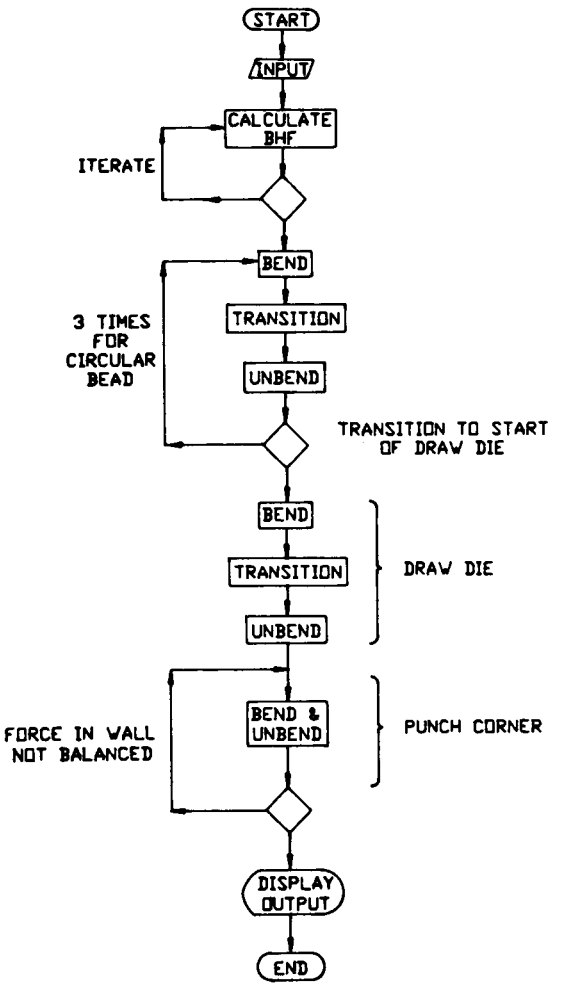


**Fig. 2.** Schematic of DRAWBD.

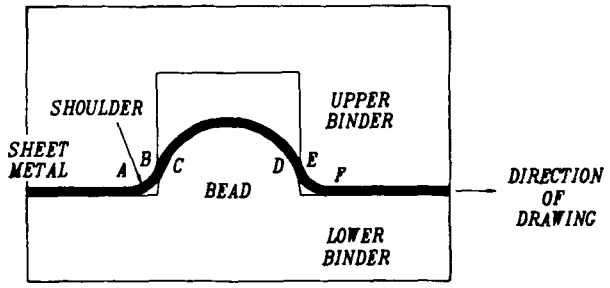


**Fig. 3.** Schematic of a drawbead.

radius. Nine's experimental work [4] indicated that this assumption is well justified. The first step starts where the flat sheet at A bends to conform to the blankholder radius. Then the sliding operation between A and B takes place under the effect of Coulomb friction, with no associated thinning. This is then followed by unbending at B. There are altogether three bends and unbends in a round bead. Similarly for a square bead, there exists four bending and unbending operations.

The change in the shape of the stress distribution, at the end of each of the three bending and unbending operations in the material passing the drawbead, as calculated by DRAWBD, is illustrated in Figures 4(a) through (f). The figures show the increase in tension with the progress of the bending, sliding and unbending. The five lines in the figures indicate the five steps of numerical bending and unbending. The figures illustrate the reduction in the material thickness and the change in the location of the neutral axis. The figures also demonstrate the incremental increase of the total strains at the outer fibers during bending and unbending, while the central fibres are subject to minor straining. In addition the figures show the increase of the bending moment at the start, and then its levelling at the end.

If the same material element goes through the die radius, then the extent of material thinning and increase in tension and stress distribution becomes more pronounced, as seen in Figures 5(a) and (b). Figures 6(a) and (b), on the other hand, show the stress and

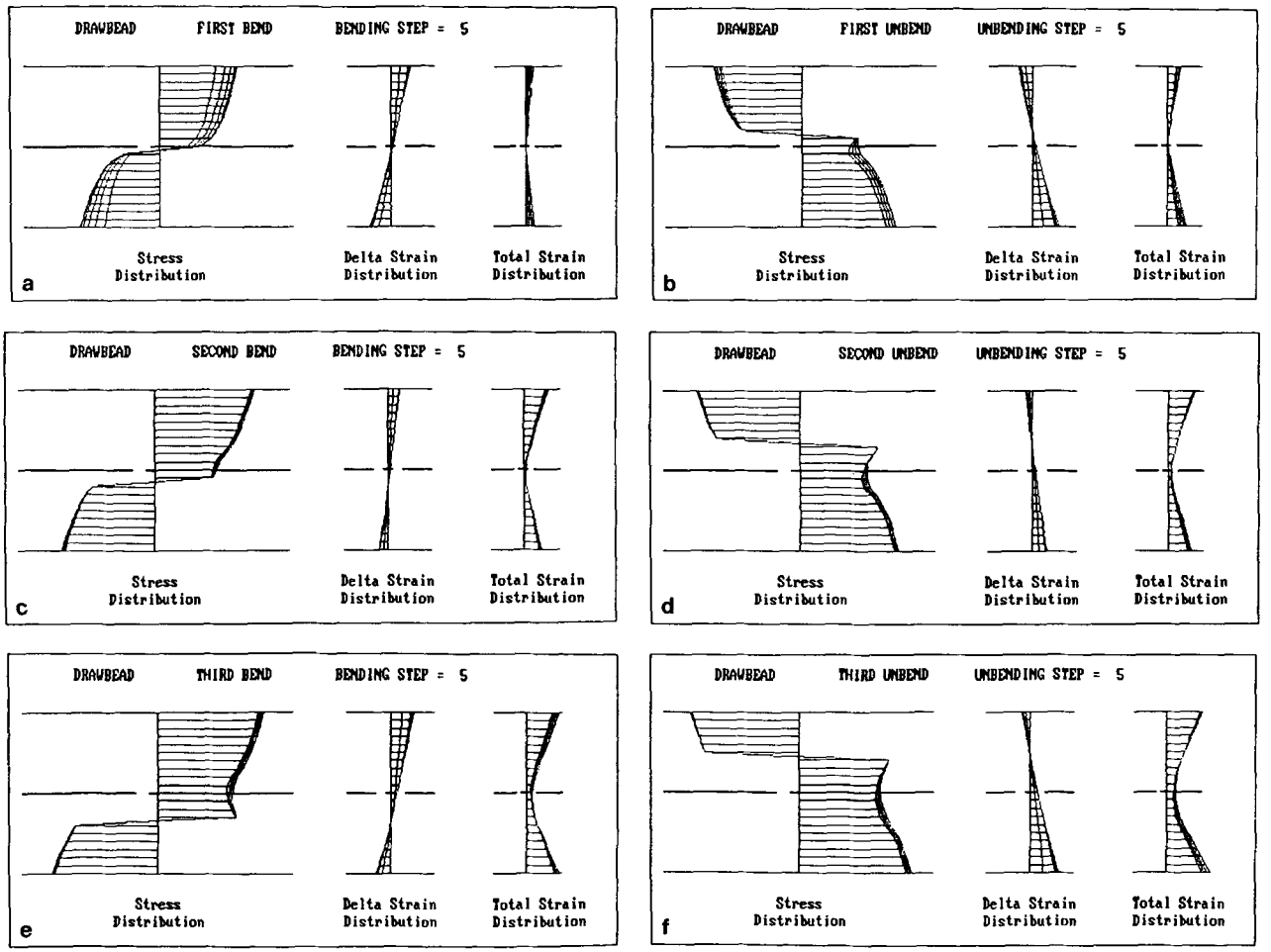


**Fig. 4.** Stress and Strain distributions at: (a) the end of first bend, (b) the end of first unbend, (c) the end of second bend, (d) the end of second unbend, (e) the end of third bend, (f) the end of third unbend.

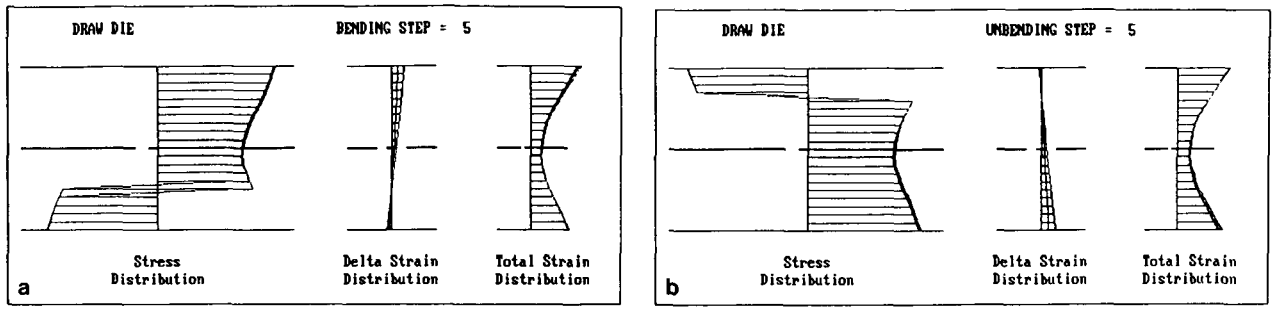


**Fig. 5.** Stress and strain distributions during the: (a) bending process, (b) unbending process, around draw die.

strain history for a material element that started in the flange in the front of the bead, and was subject only to the bead restraining force. In this case, and as expected, the material element is subject to less thinning and to a lower level of resulting bending moment. The levels of the normal force (tension) and bending moment have a major impact on the springback of the part.

The level of tension for the material passing the draw radius sets up the tension at the punch contact. The punch profile radius and the coefficient of friction then dictate the amount of material thinning and normal stress distribution over the punch face; assuming a plane strain mode of deformation. The results of the calculations are illustrated in Figure 7. These indicate that for punch profile radii larger than die profile radii, the tension on the punch face is usually larger than the tension in the flange. Figure 7 also shows the excessive shift of the neutral axis, for the material element at the punch contact, as compared to the elements in the wall. The thickness (left), tension (top right), and stress (bottom right) distributions as the material passes the bead, and then enters the die cavity are shown in Figure 8. Details of the calculations are given in Table 2.

The results for the bead restraining force, bending moment, and thickness distributions compare reasonably well with the work of Wang [7]. Figure 9 shows that the thickness distribution calculated by DRAWBD agrees well with that from Nine [4]. However, slight deviations of the drawing force occur when compared with the experimental results of Nine [4, 5]. A summary for the comparison with the experiments of Nine [5] is given in Table 3. The results in Table 3, for the drawbead restraining force (DR), are based on the experimental values of the blankholding force (BH), and the reported coefficients of friction in [5]. Higher drawing forces of 2036-T4 are obtained from DRAWBD as compared with the result of Nine. However, the reverse is true for the two types of steel used. Some possible reasons for the discrepancy can be due to strain rate effects and cyclic loading that were not accounted for in this model. Another possibility is the effect of friction. Friction results reported by Nine [5] are average for the three bends and unbends over the whole drawbead. Table 4 illustrates that when the coefficient of friction with the AK steel is varied around the blankholder corners and the drawbead by approximately +/− 10%, the drawing load through the bead is affected by only 2% according to DRAWBD. However, for the rimmed steel under same blankholding force, when the coefficient of friction is increased to 0.24, DRAWBD predicted the same drawing load as Nine's experiments [5]; refer to Table 4 for more detail. The results in Table 3 indicate that closer agreement, for steels, is obtained for the case of rollers instead of fixed drawbeads and the error increases with the increase of the coefficient of friction. The reverse is true for the case of 2036-T4. Since with increased friction the level of straining and

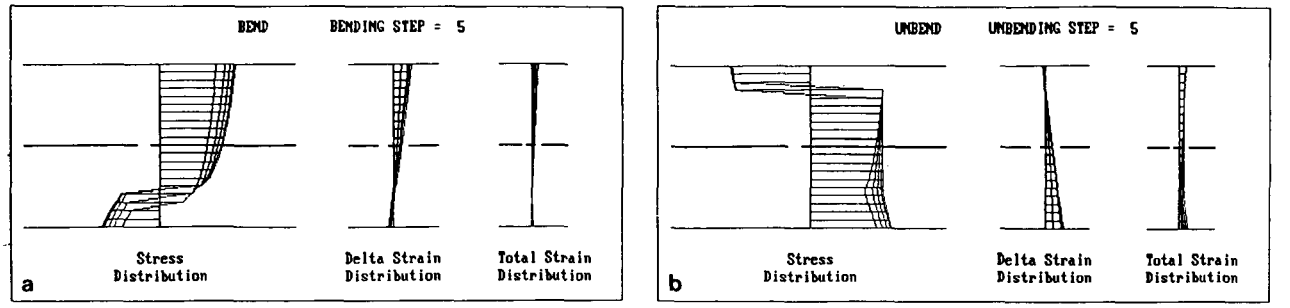


**Fig. 6.** Stress and strain distributions of an element that started (a) after bead at end of bending at die corner, (b) after bead at end of unbending at die corner.

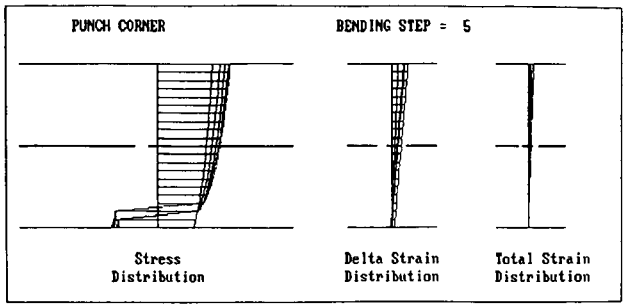


**Fig. 7.** Stress and strain distributions of an element during bending around punch corner.

hardening increases, DRAWBD results could therefore indicate a deficiency of the model due to the mode of hardening; the model assumes isotropic hardening. The deviations of the drawing force might also be due to the usage of the mechanical properties at a different strain rate than those used in drawbead experiments [5]. Figure 10 shows the DRAWBD's steady-state restraining load prediction, as compared to the numerical model of Triantafyllidis et al. [12] and the experiments of Maker et al. [13]. As seen, DRAWBD predictions compare reasonably well with experiments.

## FORMABILITY AND UNIFORMITY IN TOOLING DESIGN AND OPERATION

The sheet metal engineering stamping process is a highly interactive system. The five major aspects that influence the formability of the part are the material, geometry of part, the process, the tooling, and the tribological system. Some of these parameters, within a system perspective, have been addressed in the experimental investigations presented by Keeler et al. [15], and Straßburger et al. [16].

The discussion in this section is aimed at illustrating the effects of *tooling* and *operational* changes on the characteristics of the formed part, and accordingly quantify the difference between the problems of *formability* as opposed to *uniformity*. The simulation applies to parts in which the forming is mainly controlled by drawbeads.

The simulation is carried out using the DRAWBD program, and all comparison will be in reference to the case, with input shown in Table 1, and with reference to the results given in Table 2. This case will be referred to as *reference*. The whole process of forming including drawbead parameters, punch and die parameters, material parameters, as well as tooling setup, is examined within a system's perspective. The comparison, with the reference case, is based on thickness distribution along the part, tension in side wall, stress distributions at different sections, tension and bending moment. The comparison is based on the evaluation of material yielding over punch face, before reaching the die profile radius, as well as on the possibility of splitting for elements stressed above the level of the ultimate tensile stress, in plane strain. In addition, the limit of formability of the material can be evaluated. The level of tension and bending moment are used in a qualitative manner to estimate the effect of the stamping system on the springback of the metal.

### Tooling Adjustment Beyond Trim Line

The comparison in section is based on evaluating the adjustments beyond the trim line, and includes changes in blankholder force, bead penetration, back tension, bead and blankholder radii, as well as the usage of multiple beads.

When the blankholder force is increased by 50% (case 1), compared to the minimum requirements of the reference case, to 1080 lb/in. (18.91 N/mm), it is shown in Table 5 that the *thickness after the bead,* at the die radius, and over the punch face are marginally reduced compared to the reference case (case 0). This increased blankholder force is translated in the DRAWBD model as an increased back tension. The stress at the wall is increased by less than 6%, while the wall tension is increased by 4.7%. The result of the bending moment indicates less springback at whole section between punch and wall.

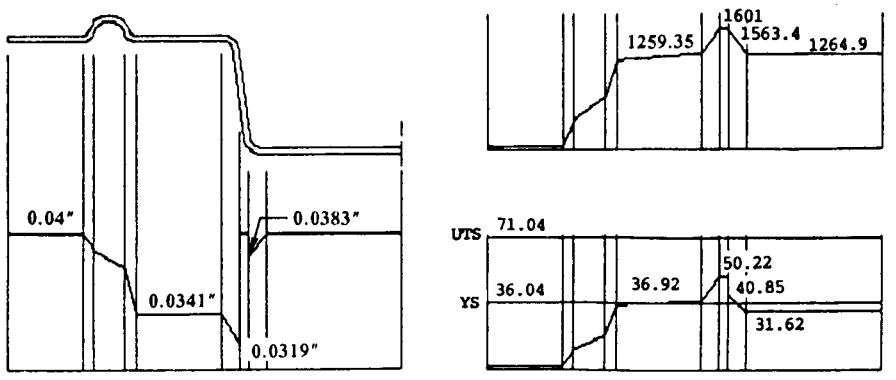


**Fig. 8.** Example of thickness, tension, and stress distributions of an element that passes through the drawbead and drawdie.

**Table 2.** Results of DRAWBD Analysis

| Solution per Unit Width | |
|---|---|
| Blankholder force | 720 lb |
| Force required to sink material in | 150.89 lb |
| Back tension | 64.98 lb |
| Thickness after passing through drawbead | 3.41E-02 in. |
| % elongation of material after drawbead | 17.28% |
| Drawing stress required through drawbead | 36.92 ksi |
| Thickness after passing draw die | 3.19E-02 in. |
| % elongation of material after draw die | 25.48% |
| Drawing stress required after passing draw die | 50.22 ksi |
| Thickness at punch contact | 3.83E-02 in. |
| % elongation of material at punch contact | 4.51% |
| Stress at punch contact | 40.85 ksi |
| Drawing stress over punch face | 31.62 ksi |

**Warning Notes by Drawbd Program:**
Drawing stress through bead exceeds the yield stress of material.
Drawing stress after draw die exceeds the yield stress of material.
Stress at punch contact exceeds the yield stress of material.

By increasing the bead penetration to 0.4 in. or 10.16 mm (case 2), the wrap angle is increased from 120 to 160 degrees. The back tension, and therefore the minimum blankholder force tension needs to be increased by 17%. This increased bead penetration has a larger effect on the stress system and springback as compared to case 1. The stresses over the punch face are, however, still within the elastic range (below the 36 ksi or 248.21 MPa equivalent yield stress in plane strain).

The increase of the back tension (case 3) by 400 lb/in. (70.05 N/mm), on the other hand, does have drastic implications on the results. In this case, the press must be set to increase the minimum blankholder force by 142%. The result is wall tension increased by 43%. The material yields extensively after the bead, and fractures after the die radius (drawing stress is larger than the 71 ksi or 489.53 MPa ultimate tensile stress value of the material in plane strain). The material over the punch face also yields, and results in drastic reduction in springback at the punch radius. This order of increase of back tension is not unexpected in practical applications. This could result from the change of blank shape, increase in blank size, or change of blank location. A simple calculation, using MIDFC [18], for a 10 in. × 5 in. × 4 in. (254 mm × 127 mm × 101.6 mm) rectangular pan with a 1 in. (25.4 mm) corner radius and 0.5 in. (12.7 mm) flange, made of 0.040 in. (1 mm) AKDQ, would indicate that the back tension would increase from 1328 (232.5) to 1520 lb/in. (266.2 N/mm) for a 0.25 in. (6.35 mm) increase of blank size, or from just changing the locator of the blank as illustrated in Figure 11. Similar conclusions were made by Siekirk [14], whose experimental observations indicated that a 1/16 in. (1.5875 mm) change in locator position could result in part failure.

The drawbead restraining force, and hence the tension in the wall, can be reduced by using a more generous bead and blankholder radii (case 4); 0.252 in. (6.4 mm) and 0.25 in. (6.35 mm) as compared to 0.25 in. (6.35 mm) and 0.125 in. (3.175 mm), respectively, for the reference case. The minimum blankholder requirement is extensively reduced by 62.5%, and results in a 40% reduction of wall tension as illustrated in Figure 12. The stress along the part becomes totally in the elastic region, which results in large springback.

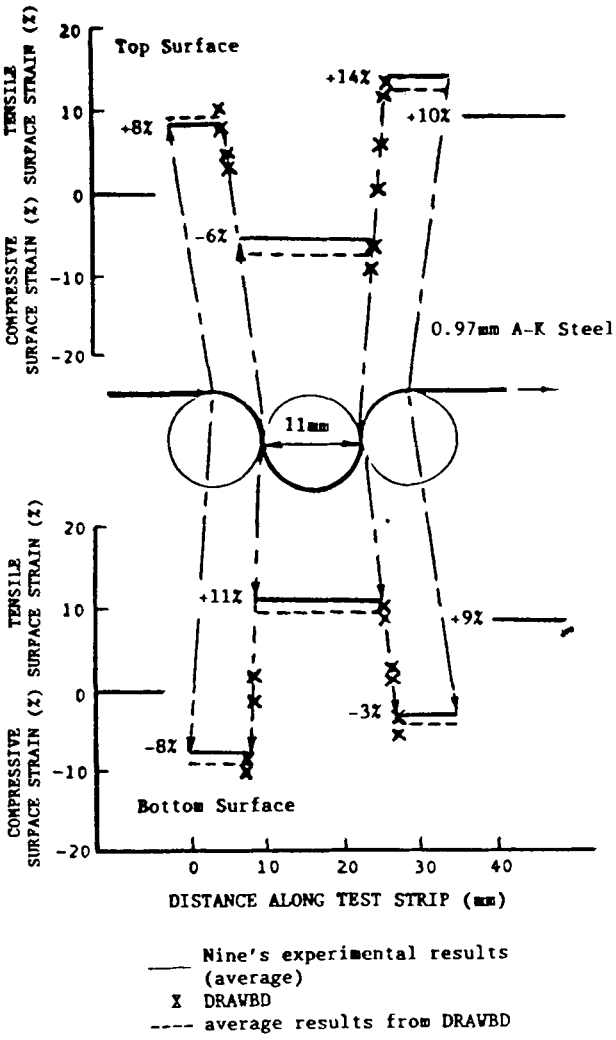


**Fig. 9.** Surface strain of a strip being pulled through a 11 mm diameter roller.

**Table 3.** Comparison of Drawbead Forces for Different Test Lubricants on Steel and Aluminum

| Lubrication Condition | Forces or μ | Rimmed Steel 0.76 mm Thickness Nine* | Rimmed Steel 0.76 mm Thickness DRAWBD | AK Steel 0.86 mm Thickness Nine* | AK Steel 0.86 mm Thickness DRAWBD | 2036-T4 Aluminum 0.89 mm Thickness Nine* | 2036-T4 Aluminum 0.89 mm Thickness DRAWBD |
|---|---|---|---|---|---|---|---|
| | | **5.5 mm Drawbead Radius** | | | | | |
| MO Lubricant | DR (kN) | 5.7 | 4.77 | 6.4 | 5.59 | 5.7 | 6.08 |
| | BH (kN) | 4.2 | | 4.8 | | 4.8 | |
| | μ | 0.18 | | 0.16 | | 0.17 | |
| Rollers | DR (kN) | 3.3 | 2.92 | 3.9 | 3.67 | 3.2 | 3.9 |
| | BH (kN) | 3.0 | | 3.2 | | 2.8 | |
| SB Lubricant | DR (kN) | 4.0 | 3.51 | 4.6 | 4.16 | 3.9 | 4.66 |
| | BH (kN) | 3.4 | | 4.1 | | 3.5 | |
| | μ | 0.07 | | 0.05 | | 0.07 | |
| | | **4.75 mm Drawbead Radius** | | | | | |
| MO Lubricant | DR (kN) | 6.3 | 5.36 | 6.9 | 6.46 | 5.9 | 6.49 |
| | BH (kN) | 4.7 | | 4.9 | | 4.7 | |
| | μ | 0.17 | | 0.16 | | 0.14 | |
| Rollers | DR (kN) | 3.8 | 3.4 | 4.3 | 4.27 | 3.8 | 4.55 |
| | BH (kN) | 3.4 | | 3.7 | | 2.8 | |
| SB Lubricant | DR (kN) | 4.6 | 3.97 | 5.3 | 5.09 | 4.9 | 5.55 |
| | BH (kN) | 3.9 | | 4.1 | | 4.2 | |
| | μ | 0.06 | | 0.07 | | 0.08 | |

*Nine's experimental results [4,5].

**Table 4.** Effect of Variation of Coefficient of Friction Around Bead Design on Drawing Force, as Predicted by DRAWBD.

| Coefficient of friction at 1st corner of blankholder | Coefficient of friction at drawbead | Coefficient of friction at 2nd corner of blankholder | Drawing force through bead |
|---|---|---|---|
| | **AK Steel (0.86 mm thick) with 5.5 mm Drawbead Radius** | | |
| 0.18 | 0.16 | 0.14 | 5.47 KN |
| 0.16 | 0.16 | 0.16 | 5.59 KN |
| 0.14 | 0.16 | 0.18 | 5.70 KN |
| | **Rimmed Steel (0.76 mm thick) with 5.5 mm Drawbead Radius** | | |
| 0.20 | 0.20 | 0.20 | 5.1 KN |
| 0.23 | 0.23 | 0.23 | 5.5 KN |
| 0.24 | 0.24 | 0.24 | 5.7 KN |

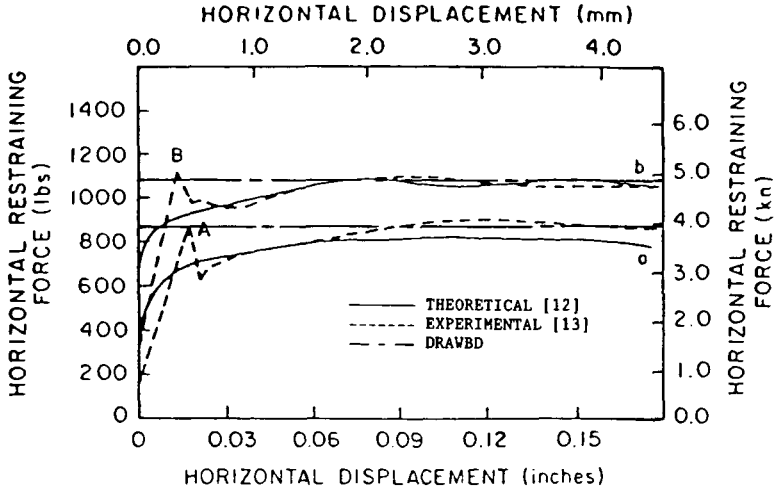


**Fig. 10.** Comparison of DRAWBD restraining force with theory of Triantafyllidis [12] and experiments of Maker et al. [13].

**Table 5.** Results of Percent Elongation, Drawing Stresses, and Bending Moment for Different Input Parameters

| Case No. | BHF (lb) | Thick. after Bead (in.) | % Elong. | Drawing Stress after Bead (ksi) | Thick. after Die (in.) | % Elong. | Drawing Stress after Die (ksi) | Thick. at Punch Contact (in.) | % Elong. | Stress at Punch Contact (ksi) | Drawing Stress, Punch Face (ksi) | Bending Moment, Die (lb-in.) | Bending Moment, Punch (lb-in.) | Wall Tension (lb) |
|---|---|---|---|---|---|---|---|---|---|---|---|---|---|---|
| Reference | 720 | 0.0341 | 17.28 | 36.92 | 0.0319 | 25.48 | 50.22 | 0.0383 | 4.51 | 40.85 | 31.62 | −14.59 | 9.74 | 1601.00 |
| 1 | 1080 | 0.0338 | 18.39 | 39.43 | 0.0315 | 27.02 | 53.23 | 0.0381 | 4.92 | 42.97 | 33.11 | −13.33 | 8.97 | 1676.26 |
| 2 | 845 | 0.0337 | 18.74 | 41.60 | 0.0313 | 27.75 | 55.92 | 0.0380 | 5.39 | 45.12 | 34.59 | −12.36 | 8.22 | 1751.00 |
| 3 | 1745 | 0.0300 | 33.27 | 64.37 | 0.0274 | 46.04 | 83.46 | 0.0353 | 13.18 | 63.60 | 45.15 | −1.71 | 2.52 | 2285.88 |
| 4 | 270 | 0.0376 | 6.48 | 17.45 | 0.0359 | 11.46 | 26.74 | 0.0390 | 2.45 | 23.82 | 18.96 | −23.53 | 15.63 | 959.74 |
| 5 | 720 | 0.0341 | 17.17 | 36.89 | 0.0298 | 34.25 | 64.25 | 0.0375 | 6.70 | 50.02 | 37.81 | −9.63 | 6.48 | 1914.43 |
| 6 | 720 | 0.0341 | 17.28 | 36.92 | 0.0319 | 25.48 | 50.22 | 0.0374 | 6.85 | 41.39 | 31.62 | −14.59 | 12.04 | 1601.00 |
| 7 | 720 | 0.0341 | 17.28 | 36.92 | 0.0319 | 25.39 | 49.10 | 0.0374 | 6.82 | 41.20 | 32.18 | −14.95 | 12.12 | 1566.35 |
| 8 | 815 | 0.0360 | 19.43 | 39.94 | 0.0334 | 28.71 | 54.39 | 0.0409 | 5.22 | 43.43 | 33.39 | −15.05 | 10.51 | 1817.14 |
| 9 | 625 | 0.0321 | 15.23 | 33.95 | 0.0302 | 22.39 | 45.93 | 0.0356 | 3.87 | 38.19 | 29.87 | −13.88 | 8.88 | 1388.47 |
| 10 | 720 | 0.0341 | 17.20 | 37.94 | 0.0319 | 25.43 | 51.50 | 0.0384 | 4.17 | 41.78 | 32.44 | −14.57 | 10.56 | 1642.48 |
| 11 | 720 | 0.0341 | 17.38 | 35.98 | 0.0319 | 25.55 | 49.03 | 0.0381 | 4.91 | 40.01 | 30.85 | −14.59 | 9.02 | 1562.11 |
| 12 | 720 | 0.0341 | 17.38 | 35.83 | 0.0318 | 25.61 | 48.70 | 0.0383 | 4.54 | 39.58 | 30.63 | −13.98 | 9.33 | 1550.90 |
| 13 | 720 | 0.0341 | 17.21 | 38.04 | 0.0319 | 25.38 | 51.76 | 0.0383 | 4.48 | 42.12 | 32.62 | −15.18 | 10.12 | 1651.43 |
| 14 | 675 | 0.0345 | 15.95 | 33.08 | 0.0324 | 23.35 | 44.02 | 0.0385 | 3.81 | 36.12 | 28.20 | −16.94 | 11.49 | 1427.59 |
| 15 | 720 | 0.0341 | 17.28 | 36.92 | 0.0319 | 25.48 | 50.22 | 0.0383 | 4.37 | 40.07 | 27.03 | −14.59 | 10.02 | 1601.00 |
| 16 | 385 | 0.0368 | 8.81 | 21.87 | 0.0355 | 12.83 | 29.00 | 0.0390 | 2.65 | 25.70 | 20.48 | −22.60 | 15.07 | 1028.13 |

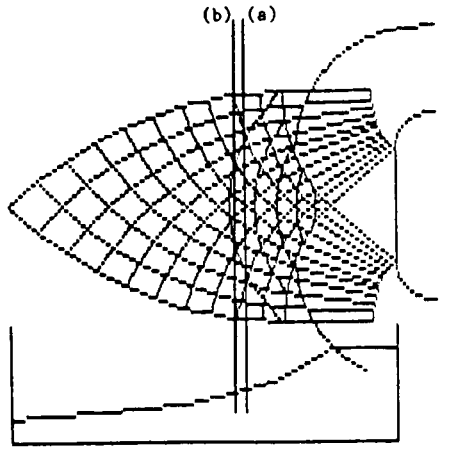


**Fig. 11.** Slip line field at the straight side of pan with the corresponding midsection velocity. Results show that an increased blank size will increase back tension and decrease edge velocity.

| | case (a) | case (b) |
|---|---|---|
| Blank size on edge | 3.572 in. (90.7 mm) | 3.822 in. (97.1 mm) |
| Back tension | 1328 lb/in. (232.5 N/mm) | 1520 lb/in. (266.2 N/mm) |
| Flange stress | 33.19 ksi (228.85 MPa) | 38.0 ksi (261.97 MPa) |
| Normalized edge velocity | 0.525 ft/min (0.16 m/min) | 0.496 ft/min (0.151 m/min) |

## Tooling Adjustment Within Trim Line

The adjustments covered below include changes of punch and die radii, as well as adjustment of tooling geometry to create a taper condition on the part wall. These represent some tooling adjustment practices to modify the formability of the part. All these adjustments would not require modification to the minimum blankholder requirements as well as the sink-in force and accordingly, will not result in changes in the thickness and the stress of material before reaching the die radius.

The use of a smaller die profile radius (case 5 with 0.125 in. or 3.175 mm die radius as compared to 0.25 in. or 6.35 mm reference) results in increased wall tension. The material in the wall and over the punch face becomes more plastic, and shows a corresponding reduction of springback.

A smaller punch profile radius (case 6 with 0.2 in or 5.08 mm punch radius as compared to 0.375 in. or 9.525 mm reference) will affect material elements only in contact with the punch and nowhere else in the wall. The adjustment in case 6 results in a smaller material thickness at the contact with the punch radius, and increased springback at the punch contact.

More material can be pulled from under the punch face when the taper of the wall is increased, as illustrated in case 7, for a condition similar to case 6, however with a 75 deg taper angle and a 0.2 in. (5.08 mm) punch profile radius. The wall tension is marginally decreased, as compared to case 6, and accordingly material springback is increased.

## Variability of Material

The simulation covered below illustrates the effect of approximately ±10% changes of the incoming material properties. These properties include thickness, strain hardening exponent, and normal anisotropy parameter.

The larger incoming material thickness (case 8) will require a larger blankholder force, and a larger bead sink-in force. Figure 13 shows the increase in wall tension with a resulting increase of bead and wall stresses and because of its thickness increase, the metal will spring back more over the punch and in the part wall. A smaller material thickness (case 9) for the same reference blankholder setup results in reduced wall tension and decreased springback at punch and wall.

The stresses induced in a more ductile material (case 11), will be marginally less than the reference case, and these would set up smaller wall forces. The material in this case is subject to slightly more thinning, and the metal springback at the punch is reduced. An opposite effect is observed with the reduction of the material ductility, as seen in case 10. The normal anisotropy of the material, as given in cases 12 and 13,

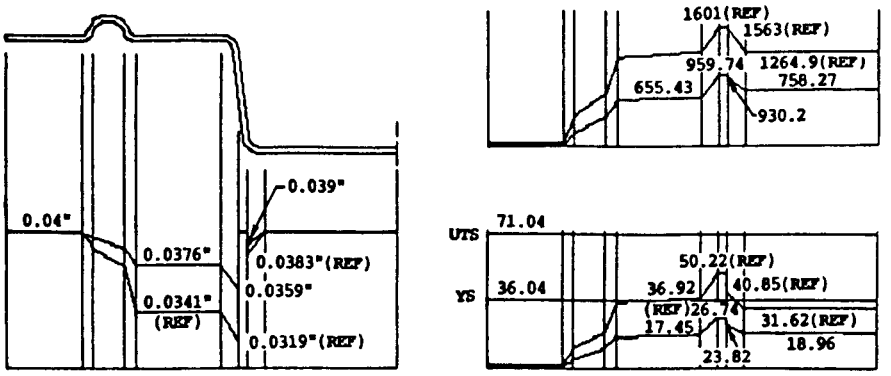


**Fig. 12.** Comparison for generous drawbead and blankholder radii of 0.252 in. and 0.25 in., respectively.

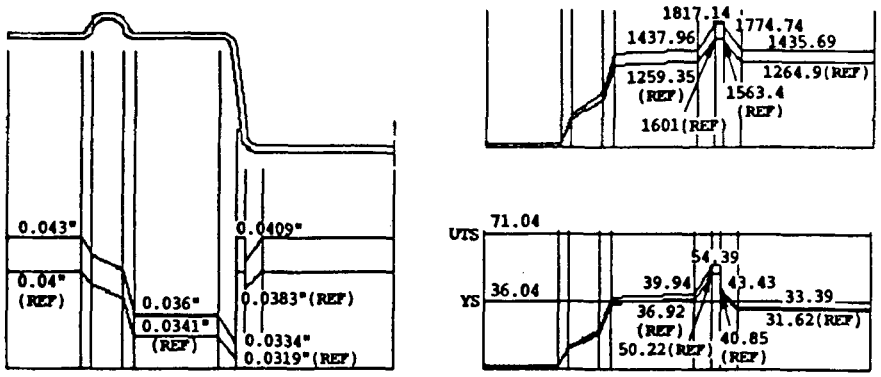


**Fig. 13.** Comparison for increased material thickness to 0.043 in.

has an opposite effect on the part formability, as compared to the strain hardening effect.

### Variability of Lubricant

The lubricant is one of the major operating parameters in a stamping plant. With a decreased coefficient of friction at drawbead and die of 0.075 for case 14, the material is subject to less severe thinning, and the wall tension is reduced by more than 10%. The stresses of the material element passing the bead, in the wall, and over the punch face are accordingly less critical. The springback of the material is, however, greatly increased as compared to the reference case. Accordingly, the state of lubricant at the die radius and drawbead has an appreciable impact on the whole part formability.

The lubricant at the punch face, however, has a localized effect around the punch, as demonstrated in case 15 of Table 5. A less efficient lubricant with a corresponding coefficient of friction of 0.25 at the punch face, would only allow slightly less material to be pulled out from under the punch face.

### Maintenance of Tooling

The following example simulates the condition of tool wear; the drawbead radius, the blankholder radius, and the die profile radius are increased to 0.252 in. (6.4 mm), 0.2 in. (5.08 mm) and 0.35 in. (8.89 mm) respectively. The results of case 16 indicate a drawbead loss of 36% of its restraining force. The material requires a smaller blankholder force to overcome the bead lifting forces. The material is also subject to less thinning and stressing, however at the expense of an increased springback of the part, and accordingly no retention of forming shape.

## DISCUSSION AND CONCLUSIONS

The design of drawbead controlled systems requires a great deal of experience. In many applications, it is not known in advance whether one or multiple beads, or even a drawbead is required. It is only at the prototyping stage that the final decision on the bead requirements is formalized.

Most of the cases described in Table 5 represent realistic variability in tooling and operating parameters. The numerical simulations described above illustrate the difficulty of empirical design of beads. In many applications, the beads are used as a means to create a wall tension that would control the material in the wall and over the punch face. For these tension controlled applications, the bead design should be based on supplying the appropriate level of tension in the wall and over the punch face. This information, on tension requirements, can be calculated in advance for the material and geometry in question. The tension at the walls can sometimes be supplied by the die profile radius without the need for drawbeads, as observed in practice for some steel bumper applications. The bead design and the tooling setup should also provide means for accommodating, when possible, the variability of the material, lubricant, process, press, and maintenance requirements.

The part response to any process change is demonstrated by a change in the thickness distribution, springback, residual stresses, etc. The results of this work showed quantitatively the effect of tooling adjustments on thickness distribution, and described the effect on springback in qualitative terms. Current efforts at Ontario Centre for Advanced Manufacturing (OCAM) are geared toward predicting in quantitative terms the effect of process and tooling adjustments on the springback and bow of the part sections. The response of the part is affected by tooling adjustments beyond the trim line, variability of material, and variability of lubricant, as well as any adjustments within the trim line. This makes troubleshooting of a production problem a most challenging task. Accordingly, process windows as opposed to material variability windows should be identified and formalized.

The results of these simulations also shed some light on the type of interaction that should exist between (a) the tooling designer and die builder who have to build means of accommodating the largest possible

window of forming, (b) the die setter and press operator who have to identify the possible window of adjustment without major changes to the tooling geometry, (c) the maintenance personnel who make the decision on when to rebuild or just replace the bead system as well as (d) quality control personnel who have the responsibility of identifying material variability versus process windows.

Despite the thin shell assumptions and the many other assumptions made in the formulation of the DRAWBD program, the following conclusions can be derived from the work presented in this paper:

1. Any tooling adjustment beyond the trim line has a direct impact on the formability of the whole part, similarly for the die profile radius adjustment.
2. Any tooling or lubricant adjustment at the punch face, has only a localized effect on the part.
3. The simulations indicate that the interactions of the different tooling and operating parameters are very complex, and accordingly the goal should be toward maintaining control over the different parameters as opposed to trying to improve on some of them. The goal should therefore be *uniformity* and *consistency* of each parameter.
4. The back tension, as reflected by shape, size, and location of blank outside the trim line, is one of the most important parameters to control, as it has a major effect on the part formability.
5. Since tooling wears in production, it is imperative that some form of qualitative and quantitative perception of the variable's interactions be made, to accommodate the variability in tooling, lubricant, and material.

## REFERENCES


1. V. Hasek: Uber den Formanderungs-und Spannungszustand beim Ziehen von grossen und unregelmassigen Blechteilen Berichte Inst. Umformtechnik TH Stuttgart nr 25, 1973.
2. M. Kojima, C. Sudo, and Y. Hayashi: "Effectiveness of Flange Holding on the Die Surface with Draw Beads," 9th Biennial Congress International Deep Drawing Research Group, 1976, pp. 207–219.
3. C. Weidemann: "The Blankholding Action of Draw Beads," 10th Biennial Congress International Deep Drawing Research Group, 1978, pp. 79–85.
4. H.D. Nine: "Drawbead Forces in Sheet Metal Forming," *Mechanics of Sheet Metal Forming,* N.M. Wang (ed.), Plenum, New York, 1978, pp. 179–207.
5. H.D. Nine: "SHAPEMATE—An Insertable, Adjustable Force Drawbead," SAE paper no. 880212.
6. H.D. Nine: "The Applicability of Coulomb's Friction Law to Drawbeads in Sheet Metal Forming," *J. Applied Metalworking,* vol. 2, no. 3, July 1982, pp. 200–210.
7. Neng-Ming Wang: "A Mathematical Model of Drawbead Forces in Sheet Metal Forming," *J. Applied Metalworking,* vol. 2, no. 3, July 1982, pp. 193–199.
8. R. Hill: *The Mathematical Theory of Plasticity,* Oxford University Press, 1950.
9. T. Furubayashi, H. Misaka, S. Ujihara, and T. Sakamoto: "The Simulation of Forming Severity on Autobody Panels Using a CAD System—Behavior of Materials after Passing the Drawbead," 14th Bienniel Congress International Deep Drawing Research Group, 1986, pp. 363–372.
10. B.S. Levy: "Modeling Binder Restraint Using Parametric Models Based on Mechanistic Considerations," *Computer Modeling of Sheet Metal Forming Process,* N.M. Wang and S.C. Tang (ed.), 1985, pp. 177–191.
11. J.M. Yellup: "Modelling of Sheet Metal Flow Through Drawbead," 13th Bienniel Congress IDDRG, 1984, pp. 166–177.
12. N. Triantafyllidis, B. Maker, and S.K. Samanta: "An Analysis of Drawbeads in Sheet Metal Forming: Part I—Problem Formulation," *J. Eng. Material and Technology,* vol. 108, 1986, pp. 321–327.
13. B. Maker, S.K. Samanta, G. Grab, and N. Triantafyllidis: "An Analysis of Drawbeads in Sheet Metal Forming: Part II—Experimental Verification," *Transactions of the ASME,* vol. 109, 1987, p. 164–170.
14. J.F. Siekirk: "Process Variable Effects on Sheet Metal Quality," *Journal of Applied Metalworking,* vol. 4, no. 3, 1986, pp. 262–269.
15. S.P. Keeler, H.D. Nine, and J.F. Siekirk: "Formability Criteria for Selecting Sheet Metal Lubricants," SAE paper no. 880366.
16. Ch. Straßburger, K. Blumel, and W. Prange: "Interaction Between Cold Rolled Sheet Steel and Forming Process," Proceedings of the Second International Conference on Technology of Plasticity, vol. II, 1987, pp. 1253–1259.
17. J.L. Duncan and R. Sowerby: "Review of Practical Modelling Methods for Sheet Metal Forming," Proceedings of the Second International Conference on Technology of Plasticity, vol. I, pp. 615–624.
18. M. Karima and W. Tse: "MIDFC and CORNFC—User Manual," OCAM Metal Forming Report MF0007, 1988.